https://doi.org/10.5194/egusphere-2026-1369
Preprint. Discussion started: 8 April 2026

An intermediary scale setup to measure O_2 fractionation factors of aquatic biosphere

Nicolas BIENVILLE[1], Amaelle LANDAIS[1], Sarah FIORINI[2], Clément PIEL[3], Joana SAUZE[3], Benoit LEMAIRE[4], Nicolas GEYSKENS[4], Frédéric PRIE[1], Olivier JOSSOUD[1], Clémence PAUL[1], Justin CHAILLOT[1], Thomas LAUWERS[1], Simon CHOLLET[2], Samuel ABIVEN[2,5], Arnaud DAPOIGNY[1]

[1]Laboratoire des Sciences du Climat et de l'Environnement, LSCE – IPSL, CNRS, CEA, UVSQ, Université Paris-Saclay, 91191 Gif-sur-Yvette, France
[2]CEREEP Ecotron-IDF, CNRS, UMS3194, 77140 Saint-Pierre-lès-Nemours, France
[3]Ecotron Européen de Montpellier (UAR 3248), CNRS, Université de Montpellier, 34980 Montferrier-sur-Lez, France
[4]INSU Division Technique, CNRS, 91191 Gif-sur-Yvette, France
[5]Laboratoire de Géologie de L'ENS, ENS-PSL, CNRS, IPSL, 75005, Paris, France

Correspondence to: Nicolas Bienville (nicolas.bienville@lsce.ipsl.fr)

Abstract. Earth atmospheric O_2 is mainly produced by biosphere photosynthesis, and biosphere respiration is also one of the main consumers of this gas. The evolution of the elemental and isotopic composition of atmospheric O_2 is thus linked to global biosphere productivity. Quantitative interpretation of the isotopic composition of O_2 in the past as archived in polar ice cores relies on robust estimates of oxygen fractionation factors associated with the relevant biological processes: photosynthesis and respiration. In the past decades, some determinations of these biological fractionation factors were performed in uncontrolled large-scale environments or at the scale of the micro-organisms in conditions very different from the natural environment. This leads to uncertainties in the applicability of these determinations for the interpretation of isotopic composition of atmospheric O_2. In order to come up with coherent estimates of oxygen biological fractionation factors applicable to the scale of plants or ecosystems, we developed a set-up of 4 closed biological chambers as a scaled-down replica of aquatic biosphere, with controlled environment parameters, and measured the evolution of O_2 concentration and of its isotopic composition. We present here 3 measurement series using this set-up run with the freshwater species *Chlorella vulgaris* and lasting between 2 and 9 months. These measurement series enabled us to validate and optimise our newly developed system for aquatic closed biological chambers. We also determined the isotopic discrimination associated with $^{18}O/^{16}O$ of O_2 during respiration as -30 ‰ which is in the upper part of the distribution of the previously published values.

1.Introduction and scientific context

The UN considers climate change the biggest threat facing humanity (United Nations, 2022). Against this threat, the biosphere is crucial because it may in part counteract the main cause of the ongoing climate change by absorbing carbon dioxide (Intergovernmental Panel on Climate Change, 2023) and furthermore because it plays a role in regulating the water cycle (NASA, 2025). It is thus important to better understand the relationships between the biosphere and Earth climate, and the study of paleoclimate enables us to do it in a diversity of climatic conditions.

A key proxy for the study of these interactions is atmospheric O_2, as the biosphere is indeed the main producer/source of atmospheric O_2 through the photosynthesis reaction, and also an important consumer/sink of atmospheric O_2 through the respiration process. While past atmospheric concentration of CO_2 can be directly retrieved from analyses of air bubbles trapped in ice cores and directly compared to past climate changes (Bereiter et al., 2015), atmospheric concentration of O_2 cannot easily be retrieved from ice core records because of elemental fractionation during the bubbles close-off (Harris-Stuart et al., 2024, Severinghaus and Battle, 2006). However, the isotopic composition of atmospheric O_2 archived in the air bubbles contains information related to biosphere activity (Bender et al., 1994; Luz et al., 2000).

https://doi.org/10.5194/egusphere-2026-1369
Preprint. Discussion started: 8 April 2026

The variations of the isotopic composition of atoms in molecules of a given sample are often expressed using the widely accepted **δ** notation. For oxygen, it is defined as follows:

$$\delta^{18}O = \frac{^{18}R_{sample} - {}^{18}R_{standard}}{^{18}R_{standard}} \quad (1)$$

with $^{18}R = {}^{18}O/{}_{16}O$

δ is usually expressed in ‰ for reading clarity.

The variation of isotopic composition is due to isotopic fractionation which occurs when the isotopic ratio of an element is modified through a process (physical, chemical, biological, …). For a reaction where the element is transmitted from a substrate to a product, this fractionation can be characterised by the fractionation factor α defined in Eq. (2):

$$^{18}\alpha_{S>P} = \frac{^{18}R_P}{^{18}R_S} \quad (2)$$

Where S is for the substrate, P for the product, and ^{18}R the isotopic ratio as previously defined (using the same formalization as Hayes, 2002). As this factor is often very close to 1, we also often use the discrimination factor $\varepsilon = \alpha - 1$. When the product of the reaction is depleted (resp. enriched) in the heavier element, $\boldsymbol{\varepsilon}$ is negative (resp. positive).

Morita et al. (1935) and Dole et al. (1935) measured the isotopic ratio $^{18}O/^{16}O$ of present-day atmospheric O_2 vs the isotopic ratio $^{18}O/^{16}O$ of the VSMOW standard (Vienna Standard Mean Ocean Water, which has a composition representative of the present-day ocean) and found a value for atmospheric $\delta^{18}O$ larger than 22 ‰. This enrichment is called Dole-Morita Effect, or commonly Dole effect (DE) and defined as follows:

$$DE = \delta^{18}O_{atm} - \delta^{18}O_{sw} \quad (3)$$

Since its first determination, the Dole Effect has been measured again several times at a value of about 24 ‰ (Kroopnick and Craig (1972): 23.5±0.3 ‰, Barkan and Luz (2005): 23.88±0.02 ‰). These positive values mostly result from the respiration process consuming the lightest isotopes and leaving in the atmosphere the heaviest isotopes (Kiddon et al., 1993). Evapotranspiration can also contribute to the positive value of the Dole effect through the process of photosynthesis. During photosynthesis, plants consume the water and transmit the $\delta^{18}O$ of the water at the site of the reaction to the $\delta^{18}O$ of produced O_2. While photosynthesis has classically not been associated with strong fractionation (Guy et al., 1993), terrestrial plants encompass evapotranspiration leading to an enrichment of leaf water $\delta^{18}O$ compared to soil water $\delta^{18}O$ and often to ocean water $\delta^{18}O$, which is then transmitted to the atmospheric O_2 during photosynthesis.

From the analyses of $\delta^{18}O$ of O_2 of the air trapped in ice cores, we know that both the atmospheric $\delta^{18}O$ of O_2 and the Dole effect varied in time, showing large variations at the precession timescale (periodicity of 21-23 ka) (Bender et al., 1994; Landais et al., 2010). The origins of these variations are still not fully elucidated but relate to the organisation of the water cycle modifying the isotopic composition of water consumed by the plants and/or to the change in the isotopic fractionation of atmospheric O_2 due to biosphere activity. To test these two hypotheses, we need a precise determination of the fractionation factors for the biological processes.

In the past decades, several studies using different set-ups and conditions tried to estimate the isotopic fractionation factors associated with the biological production and consumption of atmospheric O_2 by the aquatic biosphere. A compilation of measurements performed during field campaigns is presented in Luz et al. (2014). It shows a wide range of values: between 21.9 to 27.1 ‰ for global O_2 discrimination in the mixed oceanic layer, including fractionation effects of both oxygen uptake and photosynthesis. The extensive dataset of Reuer et al. (2007) in the Southern Ocean reported in Luz et al. (2014) shows even a larger range of values (up to 33 ‰). These values should be compared to *in vitro* determination of individual discrimination for

https://doi.org/10.5194/egusphere-2026-1369
Preprint. Discussion started: 8 April 2026

(1) ordinary or cyanide resistant respiration pathways, respectively (17.4 – 19.9 ‰) and (24.1 – 26.2 ‰) (Guy et al., 1993) and (2) photosynthesis (0 to 5.81 ‰) (Guy et al., 1993; Eisenstadt et al., 2010).

The values of the isotopic fractionation factors found by the previous studies show large variations which is expected because they were performed in different conditions and for different species. From these measurements, it is difficult to quantitatively interpret the variations of the isotopic composition of atmospheric O_2 because we first need to identify what are the main influences for explaining the broad range in the values of the fractionation factors.

During field campaigns, there is often limited knowledge about the environmental conditions prior to sampling, such as temperature, growth conditions, and the species present in the area. In parallel, the *in vitro* measurements cannot directly be applied to the interpretation of the atmospheric $\delta^{18}O$ because they were obtained in lab conditions which do not correspond to the natural conditions (e.g. no O_2 in the environment for photosynthesis). There is thus a need for performing robust and repeatable measurements in controlled conditions which are close to the natural conditions encountered on Earth.

With this objective, Paul et al. (2023) developed an intermediary scale analogue of the terrestrial biosphere consisting of vegetation–soil–atmosphere systems in closed chambers of 120L. Their study of O_2 isotopic fractionation factors gave consistent results compared with literature values for soil and plant respiration, but they calculated a non-null value of +3.7 ‰ for the photosynthesis discrimination factor. Further experimentations with this set-up included several biological chambers thanks to a multiplexed system which allowed extending their initial study to other terrestrial species and validated their finding of positive isotopic discrimination factors for photosynthesis (Paul et al. 2025a). Based on their results, they suggested that the contribution of terrestrial productivity in the Dole effect may have been underestimated in previous studies (Paul et al. 2025b).

In this study, we aim to apply a similar methodology as Paul et al. (2023, 2025a) but for the study of the biological processes of the aquatic biosphere (O_2 uptake by respiration and O_2 production by photosynthesis). We first detail the design and realisation of our aquatic biological chambers, and the environmental conditions of a first application for determining the fractionation factors of biological processes for a specific species. We then present the analytical results obtained for the different chambers detailing the evolution of elemental and isotopic composition of O_2, for several light and dark periods, as well as the calculation of the fractionation factors for the biological processes. Finally, we discuss how the newly determined fractionation factors can relate to previous values found in literature, and present perspectives for future studies using the same set-up.

2.Material & Methods

2.1.Technical development of our aquatic biosphere model

2.1.1.Requirements

First, determination of the fractionation factors of aquatic biosphere processes requires measuring the evolution of the concentration and isotopic composition of atmospheric O_2. Because changes in the isotopic composition of O_2 associated with plant biological processes are too small to be detected when measured within the huge compartment of the atmosphere (Ishidoya et al., 2025), we need to work in airtight closed biological chambers to be able to measure a non-diluted isotopic signal. Also, to obtain measurements of atmospheric O_2 truly representative of the ongoing processes, the composition of the air inside our chamber needs to be homogeneous.

Second, calculation of the isotopic fractionation during the biological processes requires frequent measurements of the elemental and isotopic composition inside the closed chamber, performed through regular air sampling. Moreover, in order to closely

https://doi.org/10.5194/egusphere-2026-1369
Preprint. Discussion started: 8 April 2026

monitor our experimental set-up and environmental conditions, our closed biological chambers should be equipped with different sensors to track the air composition and other environmental variables in real time.

Finally, as we expect large variability among biological experiments, we need to run several replicate experiments under the same environmental conditions with stable temperature, and homogeneous lighting for the photosynthesis periods. We thus used a multiplexed approach, similar to that of Paul et al. (2025a).

2.1.2.Aquatic microcosms

Our new setup is based on the aquatic microcosms already developed by the Ecotron IleDeFrance. These aquatic microcosms are composed of a round-bottom stainless steel tube of 10 cm in diameter and 88 cm in height to simulate a water column. The internal wall of the aquatic microcosm is polished like a mirror to allow light penetration from the top to the bottom, further simulating the conditions of gradient lighting in an open water column. The extinction gradient of light inside the tube is of about 50 % (80 $\mu mol.m^{-2}.s^{-1}$ measured at the bottom when receiving 450 $\mu molm^{-2}.s^{-1}$ at the top).

Water mixing, which is essential for algae growth, was ensured for each tube by 6 three-blades propellers set on a vertical rotating axis in the center of the tube. The axis was stabilised by a protruding pin at the bottom and a special stainless-steel support at the top edge of the microcosm tube. Rotation was assured by a small motor inside the instrumented module, as detailed in the following paragraph.

2.1.3.Instrumented top module

We developed a structure equipped with sensors to be adapted on the top of the tube to obtain a closed system from the open aquatic microcosms. In order to allow vertical light penetration from the above lamps, the module is built with a transparent material (polycarbonate), and all the internal instruments and sensors are deported to the side as shown on Fig. 1. Additionally to being airtight, the volume is kept small compared to the volume of the microcosm tube (about 2.5L) in order to get a strong isotopic signal from the aquatic biosphere gas exchanges.

To rotate the axis with propellers inside the microcosm, we use a small electrical motor (2232 S 024 BX SC, FAULHABER) with a speed reducer of 10. This motor is connected to the vertical axis via an angular gearbox to accommodate for the side-placed instruments.

For the homogeneity of the internal atmosphere of the chamber, we use 2 small brushless DC fans (OD3010-05MB, ORION FANS) mounted at 90° from each other. A first test showed that the atmosphere within the closed chamber is not homogeneous when using only one fan but homogeneity is ensured with the 2 fans.

To ensure that the composition of the sampled air is always the same as the composition of the air inside the closed chamber, we use a micro diaphragm gas pump (NMS020KPDC-B, KNF) to keep a loop of continuous airflow of 1.6 L/min through the sampling system. This pump is placed inside the closed chamber to avoid contamination from the outside atmosphere.

To monitor temperature, relative humidity and CO_2 concentration inside the atmosphere of the closed chamber, we use a capacitive polymer humidity sensor with an integrated PTAT (HYT 221, INNOVATIVE SENSOR TECHNOLOGY), and a non-dispersive infrared sensor (K30 3%, SENSEAIR).

https://doi.org/10.5194/egusphere-2026-1369
Preprint. Discussion started: 8 April 2026

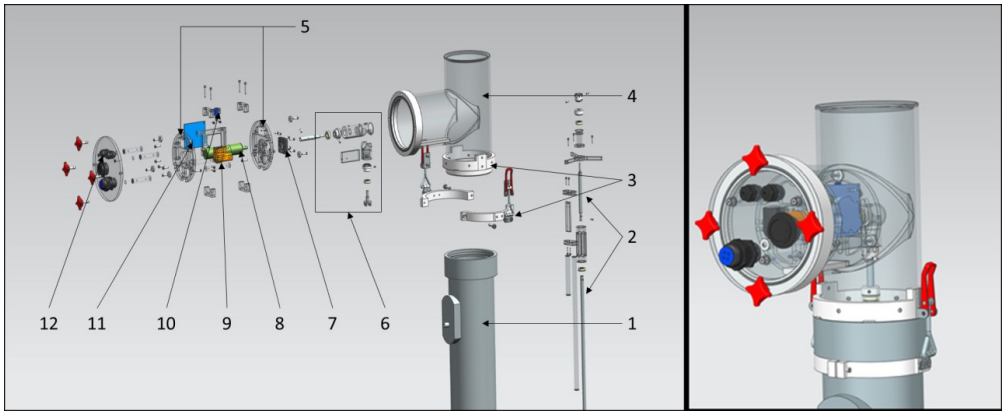

Figure 1: Exploded (left) and assembled (right) CAD views of the top module fitted on top of the aquatic microcosm tube. Legend: 1=microcosm tube, 2=vertical agitator, 3=tightening collars, 4=transparent top module, 5=structural elements with the instruments and sensors, 6=angular gearbox, 7=fan, 8=motor, 9=pump, 10=PTAT, 11=CO2 sensor, 12=pneumatic bulkheads connected to the sampling system.

2.1.4.Environmental parameters

To regulate the temperature of the tubes, we placed them inside a water tank equipped with a cryo-cooler.
The lighting was provided by a 600W lamp mounted above the set-up at an adjustable height (TOP-LIGHT HL06-600, HORTI-KING).

2.1.5.Gas sampling

As in Paul et al. (2023), the evolution of the isotopic and elemental composition has been measured by IRMS (Isotopic Ratio Mass Spectrometer) after sampling air from the system. The gas sampling setup used in our study comprises a closed loop of about 1.5m (PFA tubing, 1/4-inch) in which the air circulates thanks to the micro-pump inside the top module. This circuit is connected on the one side to the closed chamber via 2 pneumatic bulkheads (n°12 on Fig. 1, IN and OUT, Bulkhead Tube-to-Tube LF3000 Series, 6mm, Legris) and on the other side to the sampling system itself.
The sampling system is made of 2 three-way pneumatic valves for each chamber (M8.1 VBV, Rotarex) controlled by the ad-hoc experiment control software of our system. These valves are connected via two Ultra-Torr fittings (SS-4-UT-9, Swagelok, USA) to the 5mL sampling glass flasks, which are made of two Louwers HV glass valves (1-way bore 9mmRef. LH10402008, Louwers Hanique, the Netherlands) welded together. Just before being sampled inside the glass flask, the air goes through a regularly renewed cartridge of magnesium perchlorate to remove moisture.
The sampling system is also looping back to the chamber via 2 rotary valves (Valco 1/8 inch 12 positions, EUTF-SD12MWE, VICI AG International) that enable measurements of the chamber atmosphere directly online and multiplexing the different chambers with a single analyser.

2.1.6.Power and remote-control system

All communication data and power for the various instruments and sensors inside the closed chamber go through an 18 pins bulkhead connector (DD-18PMFS-QC8001, AMPHENOL LTW), and are then distributed into a circuit board designed for this purpose (Arduino Uno). This board is placed in a plastic box attached to the chamber itself. It also integrates a FireBeetle Board (FireBeetle 2 ESP32-E IoT Microcontroller, DFRobot), enabling transmission of the sensors data via Wi-Fi to the experiment control computer.
The control software has been developed using open-source Python libraries and homemade drivers to interact with the various elements (sensors, valves, etc.) through serial connections. It includes a user interface (using PyQt5 for the GUI) displaying the state of relevant components and the value of the different sensors. It also controls (1) the flask sampling system through the

https://doi.org/10.5194/egusphere-2026-1369
Preprint. Discussion started: 8 April 2026

opening and closing of the pneumatic valves enabling purge and filling of the flasks as well as (2) the flow of calibration gas and air from our biological system through the laser spectroscopy instrument for online measurement (code available at https://gitlab.in2p3.fr/olivier.jossoud/aquaoxy/-/tree/paper_2025).

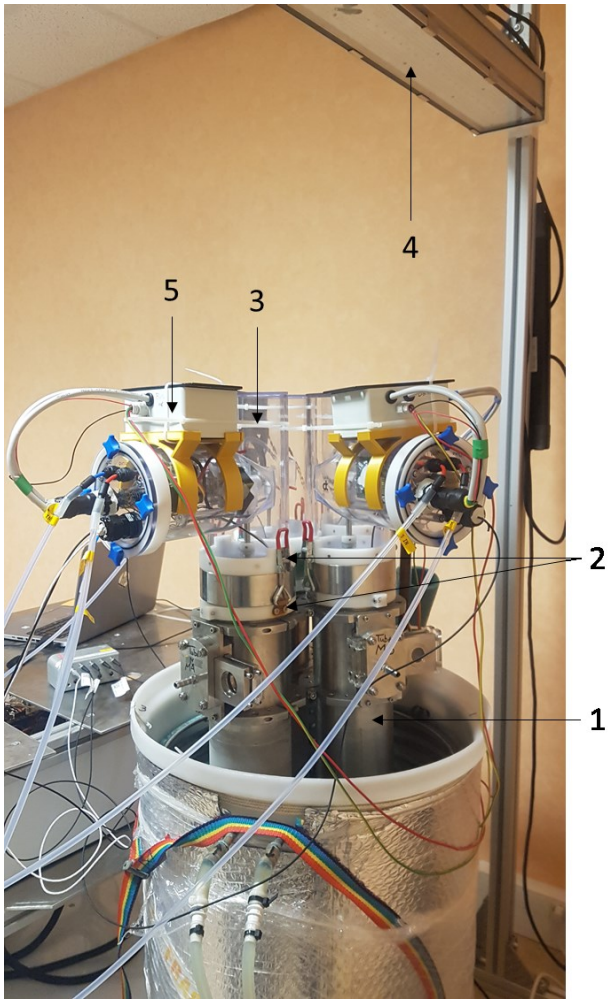

Figure 2: Picture of the setup in operation: 1=microcosm tube, 2=tightening collars, 3=top module, 4=lamp, 5=box with the control Arduino Uno.

2.2.Isotopic measurements

2.2.1.Mass spectrometry measurements

After collection of the air samples in the glass flasks, we measured their O_2 concentration and isotopic composition with an IRMS (Isotopic Ratio Mass Spectrometer) equipped with dual inlet (Thermo Delta Q, THERMOFISCHER) equipped with 8 cups to simultaneously measure masses 28, 29, 32, 33, 34, 36, 40 and 44. $\delta^{18}O$ of O_2 is calculated from the ratio of mass 34 and mass 32; $\delta O_2/N_2$ is calculated from the ratio of mass 32 and mass 28; $\delta CO_2/N_2$ is calculated from the ratio of mass 44 and mass 28.
Our sequence of measurements includes 2 series of 16 dual inlet measurements (8s of measurement of the standard, 8s of idle time, 8s of measurement of the sample, 8s of idle time). The air sample to be analysed is placed on the sample side of the dual

https://doi.org/10.5194/egusphere-2026-1369
Preprint. Discussion started: 8 April 2026

inlet and a cylinder of dry atmospheric air is placed on the standard side of the dual inlet. Every day, two samples of atmospheric air are dried and measured against the standard cylinder enabling us to check the performances of the mass spectrometer and express the isotopic and elemental composition of the sampled air with respect to the composition of the present-day atmospheric air which is the accepted standard for the isotopic composition of O_2 (Hillaire-Marcel et al., 2021; Wostbrock et al., 2020). The final precision is 1.003 ‰ for $\delta CO_2/N_2$, 0.012 ‰ for $\delta O_2/N_2$, and 0.032 ‰ for $\delta^{18}O$ of O_2.

2.2.2.Laser spectrometry measurements

Simultaneously to the discrete samplings of air from the chambers for IRMS analyses, we also aim to have continuous measurements of the elemental and isotopic composition of O_2 in every chamber in order to better follow the dynamics of the biological processes. For this, we integrate in our setup the new prototype of O_2 isotope optical analyser with OF-CEAS technology (Optical-Feedback Cavity-Enhanced Absorption Spectroscopy) described by Piel at al. (2024) and we use a similar measurement protocol as in the multiplexed system described by Paul et al. (2025).

The OF-CEAS analyser is associated with drift in the measurements so that frequent calibration is needed (~every 60 minutes) through regular switching between measurements of the air inside the chamber and measurements of a calibration gas as in Paul et al. (2025). In our case the volume of the chambers and the pressure of the analyser cavity are smaller than in Paul et al. (2025). We thus adapted the protocol by adjusting the duration of analysis to reach the desired precision (Table 1).

Table 1: Typical measurement sequence for the OF-CEAS setup.

Frequency	Phase	Phase duration (min)	Measure duration (min)	Gas source
Baseline	main calibration	60	50	dried atmospheric air
every 60 min	chamber	20	10	chamber
Once or twice a day	second calibration	20	10	dried atmospheric air enriched to 23 % of O_2 concentration

Unfortunately, because of issues with the instrument, there has been only a small period of time when we could perform some parallel measurements with this instrument integrated in the system. The results displayed in the next section were thus performed with the IRMS after sampling of the air samples in flasks, and the results obtained with OF-CEAS are presented in the supplementary materials.

2.2.3.Water isotopes

In order to calculate the fractionation factor for photosynthesis we need the isotopic composition of the water which is the substrate of photosynthesis. For this purpose, at the beginning and at the end of each experimental run, the water inside each tube is collected and its isotopic composition is analysed. This analysis of water isotopic composition is performed either with an optical spectrometer based on the CRDS (Cavity Ring Down Spectroscopy) technique (Picarro L2130-i or L2140-i), or using H_2O conversion in O_2 by fluorination followed by IRMS analyses of the isotopic composition of the resulting O_2, as in Paul et al. (2023). The precision for the measurements of the $\delta^{18}O$ of water is estimated to be better than 0.1 ‰ through replicate measurements of 10 % of the samples over the measurement period.

https://doi.org/10.5194/egusphere-2026-1369
Preprint. Discussion started: 8 April 2026

2.3.Determination of the biological fractionation factors

In the experimental setup, we measure the O_2 concentration and its isotopic composition. We detail below how to convert these measurements into the fractionation factors for respiration and photosynthesis. Note that in both calculations we do not take into account the slight fractionation at the atmosphere-water interface (Benson and Krause, 1984).

2.3.1.Respiration fractionation factor

The fractionation factor of respiration is expressed as:

$$^{18}\alpha_{respi} = \frac{^{18}R_{O2\ consumed}}{^{18}R_{O2\ initial\ air}} \quad (4)$$

Here, we work in a closed system so that during the dark periods the isotopic composition of the air in the chamber evolves only through progressive consumption of O_2 by the respiration process. We can thus use the approach of the Rayleigh distillation to link the isotopic composition of O_2 in the chamber atmosphere to its concentration. This approach is the same as in Paul et al. (2023) and we express the isotopic discrimination associated with respiration between times t_0 and t_f as:

$$^{18}\varepsilon_{respi} = {}^{18}\alpha_{respi} - 1 = \frac{ln(^{^{18}R_{O2,tf}}/_{^{18}R_{O2,t0}})}{ln\left(^{O_2,tf}/_{O_2,t0}\right)} \quad (5)$$

2.3.2.Photosynthesis fractionation factor

For the photosynthesis process, splitting water molecules to produce O_2, we express the fractionation factor as:

$$^{18}\alpha_{photo} = \frac{^{18}R_{O2\ produced}}{^{18}R_{H2O}} \quad (6)$$

Given the large size of the water reservoir, the isotopic composition of the consumed water does not vary much during our experiment, as checked through measurements of the water $\delta^{18}O$ at the beginning and end of each experiment (0.16 ‰ of standard error across all experiments).

We thus calculate the fractionation factor of photosynthesis by looking at the temporal evolution of the isotopic composition of O_2 during a period of light. Using the same equations as Paul et al. (2023) we express the discrimination associated with photosynthesis as:

$$^{18}\varepsilon_{photo} = {}^{18}\alpha_{photo} - 1 = \frac{a^{18}R + aN + {}^{18}\alpha_{respi} \times F_{respi}}{^{18}R_{H2O} \times F_{photo}} \quad (7)$$

Where $a^{18}R$ is obtained as the slope of the linear regression of ^{18}R with time ($a^{18}R = d^{18}R/dt$), and aN, F_{respi} and F_{photo} are respectively the total, photosynthesis and respiration normalised fluxes of O_2 during the light phase, expressed as

$$\left(\frac{1}{O_2, t0}\right) \times \frac{dO_2, t}{dt}$$

(with t0 being the starting time of the given light phase).

Because both respiration and photosynthesis take place during the light periods, the determination of $^{18}\alpha_{photo}$ relies on the knowledge of the respiration flux and its associated isotopic fractionation, as made explicit by Eq. (7). A simple hypothesis would be to use the same values during the light period than the values observed during the dark periods. However, Tcherkez et al. (2017) found that dark respiration could be inhibited up to 70 % in light conditions. We thus propose 2 approaches for the calculation of the discrimination factors: with either no respiration at all during the light period, or with the same mean respiration flux during the light period as during the preceding and following dark periods. The calculation with 0 % of respiration flux also

https://doi.org/10.5194/egusphere-2026-1369
Preprint. Discussion started: 8 April 2026

corresponds to the net discrimination of the light period, $^{18}\varepsilon_{light}$ rather than the one of the photosynthetic process specifically, which can be more transferrable to global Dole Effect box modelling.

2.4.First application

In order to validate our set-up, we conducted a first study with simple freshwater unicellular algae: *Chlorella vulgaris.* These algae are a widespread and representative species in regions with intense sunshine and mild temperatures. Additionally, they are fast growing algae, photoautotrophic but also mixotrophic or heterotrophic and do not form colonies. The chosen strain SAG 211-116 came from the culture collection of Algae at Göttingen University (SAG).

We have done 4 series of measurements, each starting from a new batch of algae. They are designed as "experiments" and correspond to the following periods: experiment 1 from 2024/05/30 to 2024/07/22, experiment 2 from 2024/10/22 to 2024/11/29, experiment 3 from 2024/11/29 to 2025/01/08 and experiment 4 from 2025/01/28 to 2025/10/13. For each experiment, the algae are grown in a culture medium prepared following Kilham et al. (1998) in two 5L glass bioreactors at 23 °C with a light intensity of 400 µmol $m^{-2}s^{-1}$ until a consequent cell density is reached. We then inoculate them in 3 of our biological chambers: 3L of culture were poured in each microcosm tube, completed by 3L of osmosed water, and few mL of nutrients to recreate the culture medium. A 4th microcosm is filled with water only in order to detect potential non-biological variations of O_2 concentration and isotopic composition under the same environmental conditions as in the chambers with algae.
The closed chambers are installed in a larger controlled-environment space with surrounding temperature between 25°C (1st to 3rd series) and 23°C (4th series). During the period of light, the light intensity is measured at the top of the tube to be 560 µmol $m^{-2}s^{-1}$ for each chamber. We adjusted the lengths of the dark and light periods by following the evolution of the CO_2 and O_2 concentration, changing the lighting when we observe significant O_2 and CO_2 signals (variations during a dark or light period larger than ~1000 ppm of CO_2 in at least one chamber).

3.Results

3.1.Temporal evolution of CO_2 and O_2 elemental and isotopic compositions.

Figure 3 illustrates the temporal evolution of the 3 main parameters of interest of our study (CO_2, O_2 and $\delta^{18}O$ of O_2) over one series of experiments. Results from the other series can be found in supplementary material *(Fig. S1 and S2)* as well as the results obtained with the OF-CEAS analyser.
Chamber 1 contains only water, and the 3 other chambers have the same concentration of algae culture at the beginning of the experiment. The inoculation of the algae culture into the microcosms (init "0" label on Fig. 3) occurs at least 1 week after the first filling of the tube with osmosed water. Indeed, first experiments indicate that osmosed water requires an equilibration period with the ambient atmosphere to stabilise gas exchange dynamics, particularly for stabilizing CO_2 concentration in the atmosphere of the closed chamber. After inoculation of the algae culture, we wait again about 1 week before closing the chamber to leave time for the new water - atmosphere system to reach an equilibrium. Finally, when we seal the chamber we alternate light and dark phases, represented on Fig. 3 by yellow and gray vertical bands, respectively. We sometimes open the chamber to reset the atmosphere within the chamber to the composition of the outside atmosphere.

https://doi.org/10.5194/egusphere-2026-1369
Preprint. Discussion started: 8 April 2026

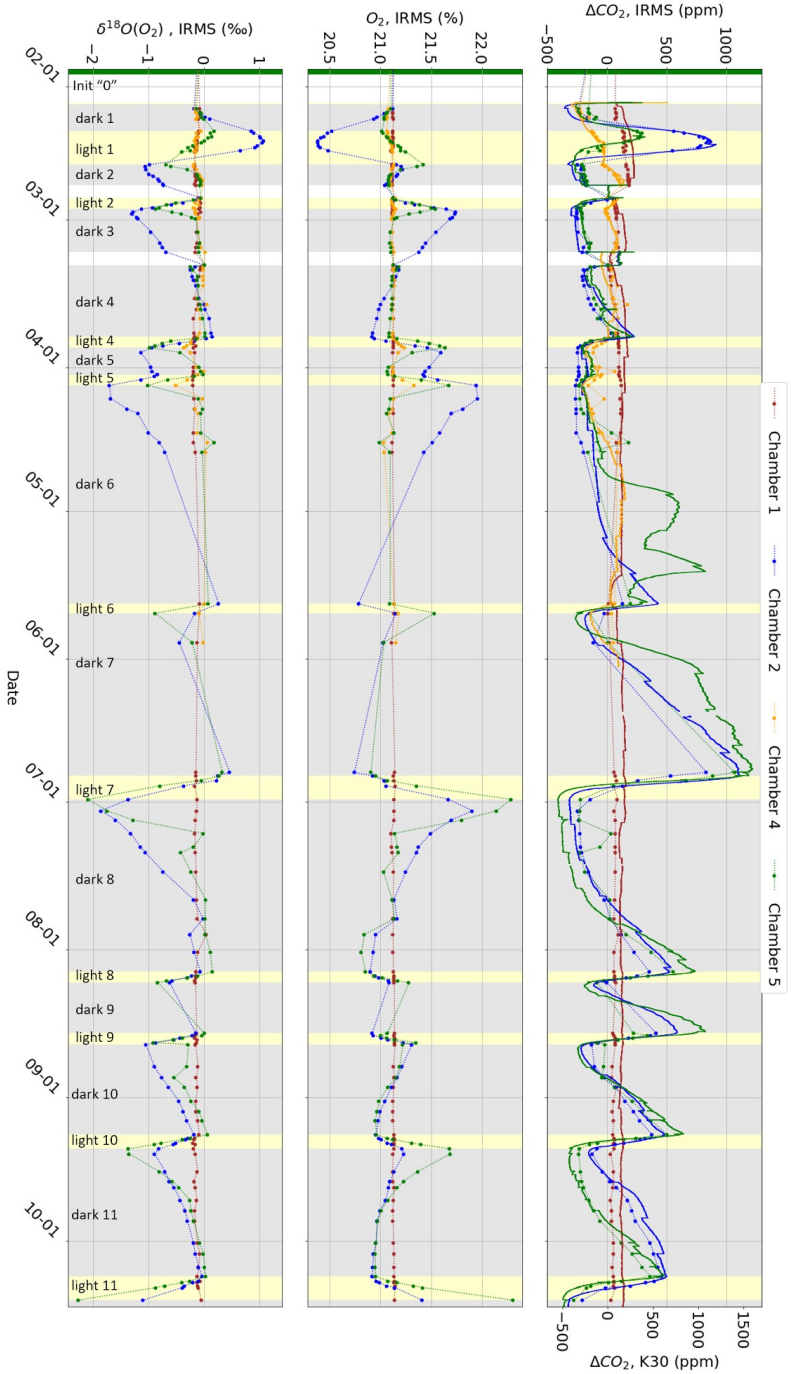

Figure 3: Evolution of CO_2 concentration, O_2 concentration and $\delta^{18}O$ of O_2 in 4 instrumented chambers over a 9-months period. The horizontal axis represents time, with the plot beginning at the injection of osmosed water into the microcosm tube. The green line (labeled "0") marks the inoculation of the algal culture into the microcosm, coloured vertical bands highlight the dark (in gray) and light (in yellow) phases. The background colour stays white when the chambers are open. The CO_2 evolution is expressed as delta values (ΔCO_2) with respect to atmospheric air concentration at the beginning of the experiment. It is measured continuously by the uncalibrated K30 sensor inside the top-module (solid line, plotted against the right-side axis) and also discretely by IRMS from the flask samplings (dotted line, plotted against the left-side axis).

https://doi.org/10.5194/egusphere-2026-1369
Preprint. Discussion started: 8 April 2026

As we can expect after the closure of the chambers, respiration causes an increase in CO_2 concentration and a decrease in O_2 concentration during the dark phases. The opposite occurs during the light phases (CO_2 concentration decreases and O_2 concentration increases) showing the dominant influence of photosynthesis, over respiration. The evolution of the isotopic composition of O_2 is also coherent with the expected fractionation processes: during respiration the algae preferentially consume the lighter O_2 isotopes, which increases the $\delta^{18}O$ of O_2 inside the chamber atmosphere. During photosynthesis the O_2 molecules generated by the algae come from the water molecules, much more depleted in heavier O_2 isotopes than atmospheric air, which decreases the $\delta^{18}O$ of O_2 inside the chamber atmosphere. The chamber with only water does not display any trend, especially for O_2 concentration and $\delta^{18}O$ of O_2, which confirms that the observed signals in the 3 other chambers are indeed biological.

When comparing the evolution in the 3 chambers containing the algae cultures, we note differences in the amplitude of the changes in O_2 concentration, CO_2 concentration and $\delta^{18}O$ of O_2 even if they all started with the same algae culture concentration. The amplitude of the changes is smaller in chamber 4 and larger in chamber 2 or 5. These differences were also observed for the other series of experiments (supplementary material).

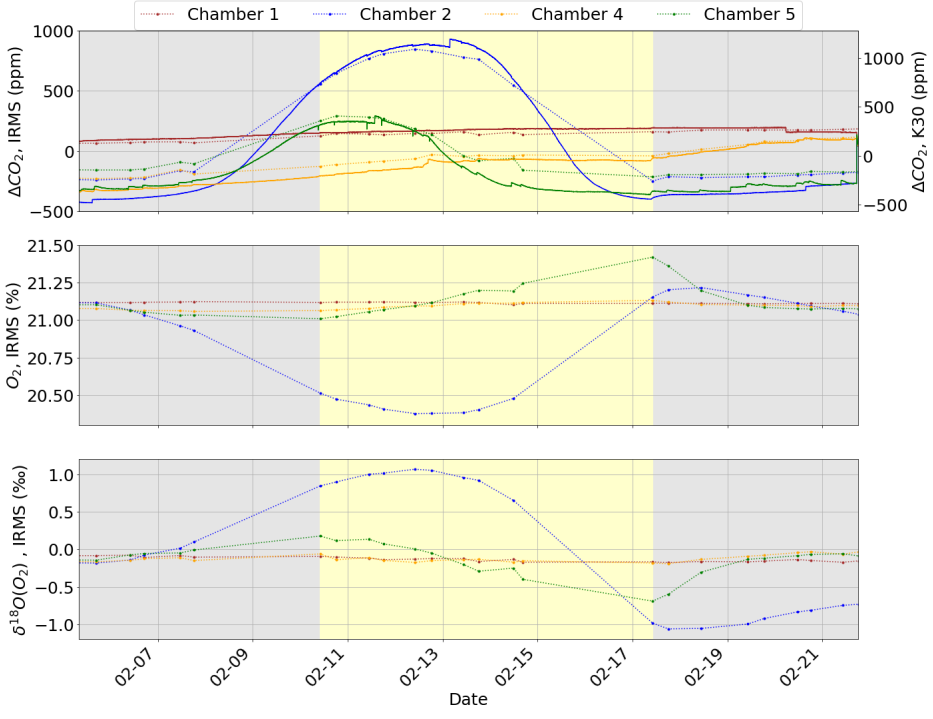

Figure 4: Same experiment as Fig. 3 with a focus on the first 3 phases (dark 1, light 1 and dark 2) to showcase the lag phenomenon.

We also observe deviation to the general pattern of respiration - photosynthesis during the first dark and light phases at the beginning of the measurement series. There is a delay between the change of enlightenment and the expected evolution of the concentrations of O_2 and CO_2. When the light is switched on after the first dark phase ("dark 1" in Fig. 3), the respiration trends do not stop immediately: CO_2 and $\delta^{18}O$ of O_2 keep increasing, and O_2 keep decreasing. This is especially the case for chamber 2, in the transition from "dark 1" to "light 1" (Fig. 3). However, on Fig. 4 we observe a change of slope for each parameter when the light is switched on: the increasing rate of CO_2 concentration and $\delta^{18}O$ of O_2 and the decreasing rate of O_2 concentration all get lower. After about 1.5 to 2 days in chamber 2 (less in chamber 5 and not visible in chamber 4), the evolution of the three parameters reaches a plateau during 2 days before an inversion of the trends now corresponding to the expected photosynthesis

https://doi.org/10.5194/egusphere-2026-1369
Preprint. Discussion started: 8 April 2026

pattern: CO_2 concentration and $\delta^{18}O$ of O_2 decrease and O_2 concentration increases. Similar lags were also observed for other batches of algae culture at the beginning of the experiments, and also stopped after the first phases.

Finally, we note that while no nutrient was added to the water since January 2025, we still observe cycles of photosynthesis and respiration 9 months later.

3.2.Discrimination factors during the dark periods

For a dark phase, with only respiration occurring, the discrimination factor is the same as for respiration ${}^{18}\varepsilon_{dark} = {}^{18}\varepsilon_{respi}$. As seen in Eq. (5), it is computed through the linear regression slope of $\ln({}^{18}R)$ vs $\ln(O_2)$. Figure 5 is an example for a typical respiration-only phase (chamber 2 phase dark 3) with a discrimination factor estimated as -28.1 ‰.

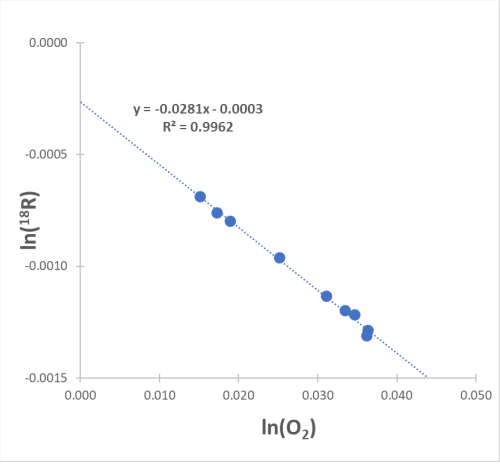

Figure 5: Example of a linear regression between O_2 concentration and isotopic composition for the phase of respiration "dark3" for chamber 2.

To assess the robustness of the calculated discrimination factors in all dark phases of our experiments, we evaluate 3 confidence parameters: the number of data points used for the regression (n), the coefficient of determination (R^2), and the amplitude of the oxygen concentration change (ΔO_2) *(more details in Supplementary)*. For the example displayed on Fig. 5, we have 9 data points (n=9), a high coefficient of determination (R^2=99.6 %) and a relatively large amplitude of the O_2 concentration (ΔO_2 = 0.4 %). Together, these parameters provide sufficient confidence in the determined slope of the $\ln({}^{18}R)$ vs $\ln(O_2)$ relationship, which directly yields the discrimination factor; its determination can therefore be considered robust. On the contrary, phases with few analytical points, low R^2 values, and/or small changes in oxygen concentration lead to discrimination factors with lower confidence and are considered less faithful. In Table 2, we systematically display the values of ΔO_2, R^2 and the number of points for each determination of the discrimination factors.

In some cases, we notice that a weak R^2 is caused by the delay observed at the beginning of the series of experiments: the change in illumination is not synchronised with the change of trend in the atmosphere composition of the chamber. In this case, we simply limit the period for the determination of the discrimination factor to the period where the expected signal of O_2 decrease is observed. All confidence parameters are then recalculated after the period adjustment, and Table 2 presents the final results of our calculation. Discrimination factors with all 3 parameters at high confidence (Table 2) represent 52 % of total values and lead to an average discrimination factor of -30.8±5.5 ‰ (1$\boldsymbol{\sigma}$).

https://doi.org/10.5194/egusphere-2026-1369
Preprint. Discussion started: 8 April 2026

Table 2: Discrimination factors calculated for the dark phases of our series of experiments, for our 3 chambers. For each dark phase we display: the date and time boundaries of the phase, the calculated discrimination factor ($^{18}\varepsilon_{dark}$) and evaluation of the 3 associated confidence parameters (n, R^2 and ΔO_2) for each of the 3 biological chambers (ch2, ch4 and ch5). For each of the determination, the parameters leading to high confidence are in green ($n \geq 5$, $R^2 \geq 75$ %, $|\Delta O_2| \geq 0.1$ %), the parameters leading to medium confidence are in yellow ($n = 4$, 50 % $< R^2 <$ 75 %, 0.02 % $< |\Delta O_2| <$ 0.1 %), and the parameters leading to low confidence are in pink ($n \leq 3$, $R^2 \leq 50$ %, $|\Delta O_2| \leq 0.02$ %).

		Chamber 2				Chamber 4				Chamber 5			
Phase label	Duration (days)	$^{18}\varepsilon_{dark}$	n	R^2	ΔO_2	$^{18}\varepsilon_{dark}$	n	R^2	ΔO_2	$^{18}\varepsilon_{dark}$	n	R^2	ΔO_2
dark α	6.8	-0.012	3	98.95%	-0.593%	-0.026	3	81.23%	-0.092%	NA	NA	NA	NA
light α	1.1												
dark β	2.1	-0.023	5	90.15%	-0.186%	-0.035	5	99.63%	-0.213%	-0.034	5	46.06%	-0.060%
light β	1.0												
dark a	1.7	-0.026	5	94.20%	-0.259%	0.020	5	7.27%	-0.016%	-0.034	5	95.95%	-0.375%
dark b	3.1	-0.030	8	95.72%	-0.055%	0.009	8	0.98%	-0.023%	-0.035	8	99.16%	-0.387%
light b	5.0												
dark d	2.9	-0.024	7	57.93%	-0.004%	-0.002	7	0.75%	-0.034%	-0.024	7	94.11%	-0.393%
light d	7.4												
light e	8.0												
dark f	1.9	NA		NA		NA	NA	NA	NA	-0.030	5	92.58%	-0.061%
light f	1.1	NA		NA									
dark g	5.2	NA		NA		NA	NA	NA	NA	-0.033	6	96.37%	-0.182%
dark 1	4.7	-0.029	6	99.66%	-0.601%	-0.035	6	13.38%	-0.013%	-0.048	6	74.41%	-0.093%
light 1	7.0												
dark 2	4.3	-0.034	9	96.71%	-0.116%	-0.053	5	84.01%	-0.034%	-0.030	9	99.66%	-0.345%
light 2	2.3												
dark 3	9.1	-0.028	9	99.66%	-0.269%	-0.020	9	6.81%	-0.015%	-0.029	9	99.63%	-0.438%
dark 4	15.0	-0.023	11	96.54%	-0.245%	0.024	12	4.44%	-0.010%	-0.045	11	90.72%	-0.096%
light 4	2.3												
dark 5	5.7	-0.026	5	96.58%	-0.042%	-0.041	5	81.44%	-0.114%	-0.027	5	99.59%	-0.567%
light 5	2.3												
dark 6	45.8	-0.028	8	99.02%	-1.159%	-0.030	8	84.32%	-0.200%	-0.028	8	97.19%	-0.579%
light 6	2.0												
dark 7	34.1	-0.032	4	65.64%	-0.230%	NA	NA	NA	NA	-0.031	4	92.63%	-0.579%
light 7	4.9												
dark 8	36.2	-0.032	12	89.50%	-0.775%	NA	NA	NA	NA	-0.026	12	95.56%	-1.437%
light 8	2.2												
dark 9	10.6	-0.047	2	NA	-0.167%	NA	NA	NA	NA	-0.066	2	NA	-0.212%
light 9	2.3												
dark 10	18.9	-0.040	8	98.58%	-0.353%	NA	NA	NA	NA	-0.028	7	68.46%	-0.231%
light 10	3.0												
dark 11	26.8	-0.043	12	97.54%	-0.292%	NA	NA	NA	NA	-0.030	12	98.97%	-0.732%

As already apparent on Fig. 3, Table 2 confirms the differences in the amplitude of ΔO_2 between the chambers. Chamber 4 is associated with low values for ΔO_2 which suggest either a very low biological activity or a leak from outside air to this chamber. While the low fluxes can already be a problem because they increase the impacts of measurement variability in the final calculated results (as seen by the low R^2 associated), we also further investigated in the discussion and supplementary materials what would be the direct impact of a leak on the calculation of fractionation factors. Finally, Fig. 6 shows that the variability of $^{18}\varepsilon_{dark}$ values decreases when ΔO_2 amplitude increases. This emphasizes the importance of long dark phases to get a robust determination of $^{18}\varepsilon_{dark}$.

https://doi.org/10.5194/egusphere-2026-1369
Preprint. Discussion started: 8 April 2026

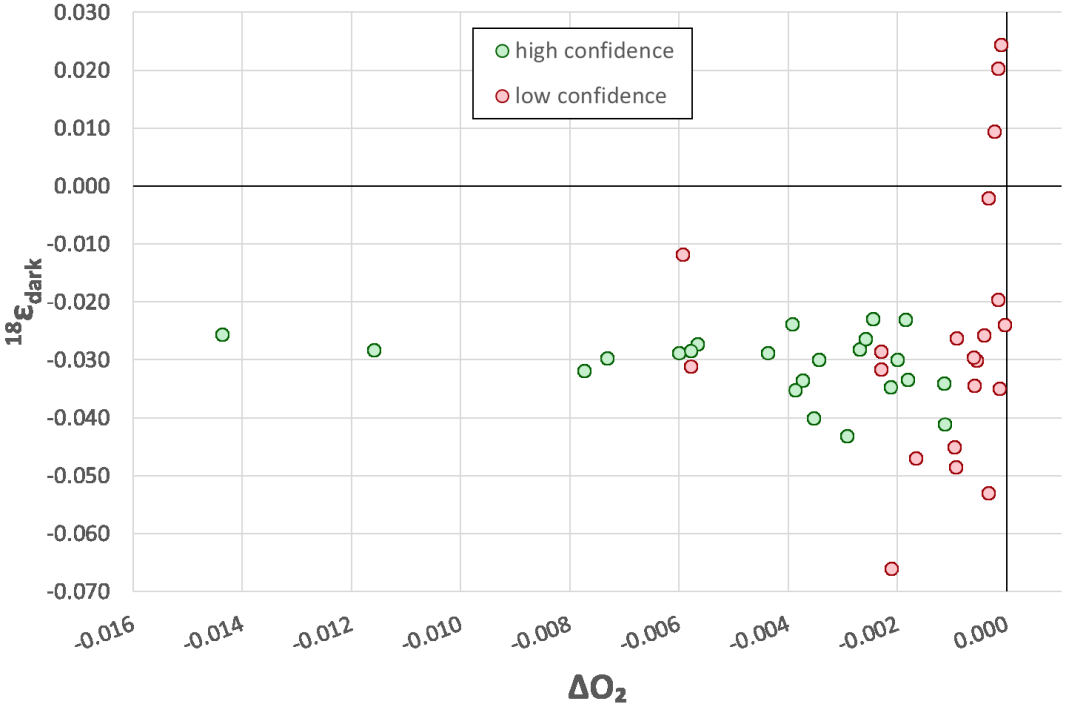

Figure 6: $^{18}\varepsilon_{dark}$ against the range of O_2 concentration decrease during the dark periods

3.3.Discrimination factors during the light periods

For photosynthesis the determination of the discrimination factor cannot be obtained from a simple regression line as for respiration, since we also need to incorporate the isotopic composition of the water, as well as the effect of the respiration on the elemental and isotopic composition of O_2 (cf Eq. (7)). However, we can use a similar approach as for respiration to evaluate the confidence in the calculated discrimination factors. We can also look at the number of data points during the light phase (n), the amplitude of the oxygen concentration change (ΔO_2), as well as the 2 coefficients of determination associated with the linear regression described in section 2.3 (R^2_{a18R} and R^2_{aN}). Table 3 presents the final results of our calculations for the 2 approaches presented in section 2.3.

Table 3: Discrimination factors calculated for the light phases of our series of experiments, for our 3 chambers. For each light phase we display: the date and time boundaries of the phase, the calculated discrimination factor assuming no concurrent respiration ($^{18}\varepsilon_{light}$), or 100 % of concurrent dark respiration ($^{18}\varepsilon_{photo}$), and the evaluation of the 4 associated confidence parameters (n, R^2_{a18R} and R^2_{aN}, and ΔO_2), for each of the 3 biological chambers (ch2, ch4 and ch5). The color code is the same as in Table 2.

https://doi.org/10.5194/egusphere-2026-1369
Preprint. Discussion started: 8 April 2026

		Chamber 2						Chamber 4						Chamber 5					
Phase label	Duration (days)	$^{18}\varepsilon_{light}$ (no respi)	$^{18}\varepsilon_{light}$ (100% respi)	n	R^2 (for $a^{18}R$)	R^2 (for aN)	ΔO_2	$^{18}\varepsilon_{light}$ (no respi)	$^{18}\varepsilon_{light}$ (100% respi)	n	R^2 (for $a^{18}R$)	R^2 (for aN)	ΔO_2	$^{18}\varepsilon_{light}$ (no respi)	$^{18}\varepsilon_{light}$ (100% respi)	n	R^2 (for $a^{18}R$)	R^2 (for aN)	ΔO_2
dark α	6.8																		
light α	1.1	-0.001	-0.001	5	99%	98%	0.290%	-0.003	-0.002	5	99%	98%	0.261%	-0.092	-0.040	3	98%	94%	0.020%
dark β	2.1																		
light β	1.0	0.004	0.003	4	98%	98%	0.339%	0.000	0.000	4	100%	99%	0.206%	-0.154	-0.086	4	35%	88%	0.033%
dark b	3.1																		
light b	5.0	-0.092	0.016	4	30%	9%	-0.011%	0.005	0.004	4	41%	97%	0.017%	-0.003	0.000	4	71%	90%	-0.203%
light c	4.9	0.030	-0.021	7	0%	54%	0.020%	-0.050	0.037	7	74%	78%	-0.009%	0.015	-0.014	7	94%	97%	-0.264%
dark d	2.9																		
light d	7.4	-0.002	-0.002	9	97%	97%	0.572%	NA	NA	NA	NA	NA	NA	0.005	0.001	8	96%	98%	0.176%
dark e	3.7																		
light e	8.0	-0.056	-0.012	7	43%	38%	0.022%	NA	NA	NA	NA	NA	NA	-0.002	-0.002	11	84%	94%	0.078%
dark f	1.9																		
light f	1.1	NA	NA	NA	NA	NA	NA	NA	NA	NA	NA	NA	NA	-0.017	-0.014	4	100%	100%	0.136%
dark g	5.2																		
dark 1	4.7																		
light 1	7.0	-0.011	-0.008	5	89%	89%	0.771%	0.012	0.007	11	46%	92%	0.068%	-0.007	-0.004	11	96%	98%	0.410%
dark 2	4.3																		
light 2	2.3	-0.004	-0.004	6	98%	95%	0.509%	-0.003	-0.004	5	42%	89%	0.037%	-0.002	-0.001	6	97%	99%	0.421%
dark 3	9.1																		
dark 4	15.0																		
light 4	2.3	-0.002	-0.002	6	99%	98%	0.551%	-0.007	-0.008	6	98%	99%	0.118%	0.001	0.000	6	95%	98%	0.557%
dark 5	5.7																		
light 5	2.3	0.002	0.002	4	98%	96%	0.520%	0.000	-0.002	4	100%	99%	0.212%	0.003	0.003	4	96%	98%	0.599%
dark 6	45.8																		
light 6	2.0	0.011	0.010	2	NA	NA	0.368%	NA	NA	NA	NA	NA	NA	-0.007	-0.006	2	NA	NA	0.438%
dark 7	34.1																		
light 7	4.9	-0.008	-0.007	4	97%	93%	0.750%	NA	NA	NA	NA	NA	NA	0.001	0.001	4	99%	98%	1.335%
dark 8	36.2																		
light 8	2.2	-0.018	-0.015	5	97%	96%	0.187%	NA	NA	NA	NA	NA	NA	-0.009	-0.008	5	99%	96%	0.430%
dark 9	10.6																		
light 9	2.3	-0.008	-0.007	6	98%	96%	0.392%	NA	NA	NA	NA	NA	NA	-0.025	-0.023	5	98%	72%	0.283%
dark 10	18.9																		
light 10	3.0	-0.010	-0.009	6	98%	96%	0.256%	NA	NA	NA	NA	NA	NA	-0.003	-0.003	6	99%	97%	0.723%
dark 11	26.8																		
light11	5.0	-0.006	-0.005	6	97%	98%	0.492%							0.002	0.002	6	99%	97%	1.354%

Evaluating the results with only the high confidence parameters (green highlights in Table 3) gives us an average discrimination factor of -4.8±5.5 ‰(1**σ**) if assuming no respiration process at all, and -4.2±4.3 ‰ (1**σ**) if assuming the same respiration flux as during the neighbouring dark phases. Both determinations are negative and when we plot the different discrimination factors against the range of O_2 concentration changes, (Fig. 7) we do not observe a clear convergence of $^{18}\varepsilon_{light}$ converging toward a constant value for larger ΔO_2 values.

https://doi.org/10.5194/egusphere-2026-1369
Preprint. Discussion started: 8 April 2026

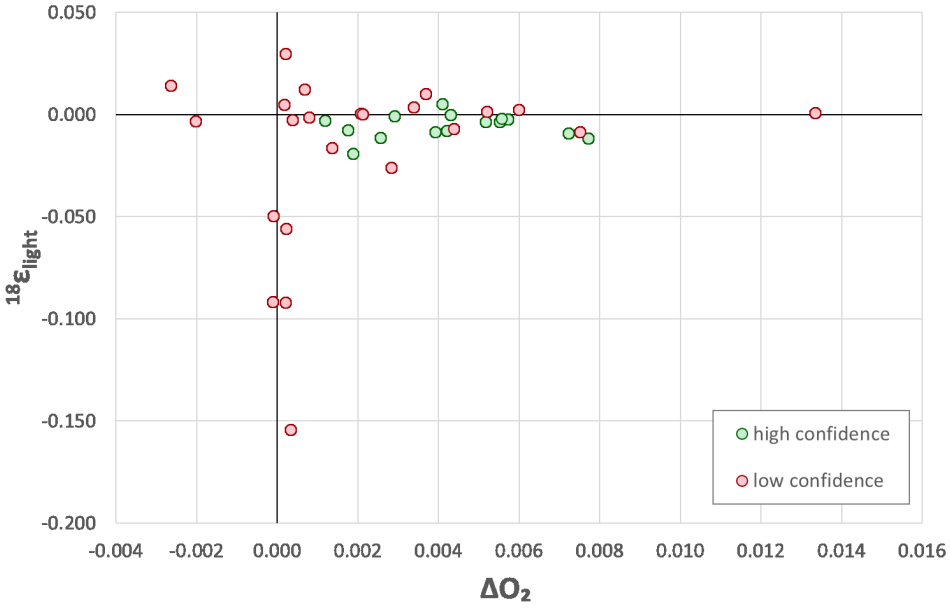

Figure 7: $^{18}\varepsilon_{light}$ against the evolution of O_2 concentration during the light phase.

3.4.Co-evolution of O_2 and CO_2 concentrations

In our set-up, we chose not to control the CO_2 concentration in the atmosphere of the biological chamber because of the liquid-air exchanges in our system. Involving only biology in the relationship between CO_2 and O_2 evolutions would lead to a ratio 1:1 between changes in O_2 number of moles and changes in CO_2 number of moles (Keeling and Manning, 2014).
Our observations (Fig. 8) actually show much stronger slopes. This is expected because CO_2 is approximately 28 times more soluble in water than O_2 (Angert et al., 2015). During algae respiration, the produced CO_2 is mainly absorbed by the water in the form of carbonic acid because of its strong polar bounds. In contrast, O_2 is barely involved in any reactions so that the consumption of dissolved O_2 is compensated by a transfer of O_2 from the chamber atmosphere into the water. The reverse effect is at play during photosynthesis: algae will consume the CO_2 present in the water and modify the equilibrium with dissolved CO_2 hence minimizing the effect on the CO_2 concentration in the atmosphere of the biological chamber. The highest slope between O_2 concentration changes and CO_2 concentration changes is observed when CO_2 concentration in the atmosphere is below 200 ppmv, hence during photosynthesis and very probably during periods when there is a lack of CO_2. This situation may be critical for the algae and should be avoided in the future through the addition of CO_2.

https://doi.org/10.5194/egusphere-2026-1369
Preprint. Discussion started: 8 April 2026

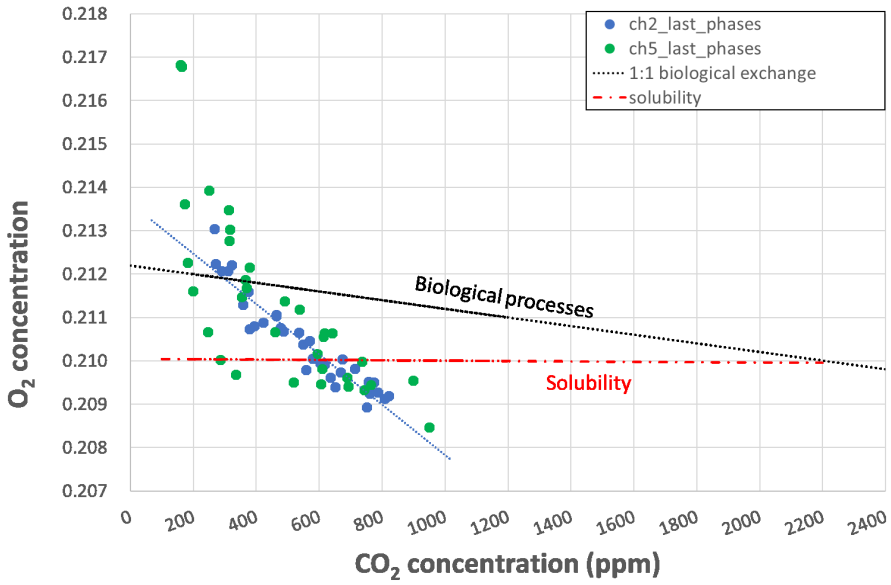

Figure 8: Evolution of O_2 vs CO_2 for several phases of the experiment for chamber 2 (in blue) and chamber 5 (in green), and slopes for biological processes only (stoichiometry O_2 vs CO_2 1:1) and for solubility (ratio O_2 vs CO_2 1:28)

4.Discussion

4.1.Evolution of the O_2 fluxes during the experiment

As written in section 3.1, we observe a lag at the beginning of the experiments between changes in lighting conditions and the corresponding response in the measured atmospheric fluxes within the chamber. Several mechanisms may explain this delay. First, solubility can play a role in delaying the change in atmospheric composition with respect to the change in the biological activity in water. As CO_2 and O_2 do not have the same solubility, we expect to see the change in O_2 concentration before the change in CO_2 concentration during light phase dominated by photosynthesis. This corresponds to our observations for chamber 5 (Fig. 4). However, in chamber 2 CO_2 and O_2 concentrations evolve synchronously during the light period, which goes against the solubility hypothesis. Moreover, if solubility alone would explain this delay, we would observe it in later phases, and not only at the beginning of the series of experiments.

An alternative explanation is the evolution of the algae cultures along the experiment. In the first phases of the experiment, algae are probably at an early stage of their development with enough nutrients still available, while algae population is sparse due to dilution at the beginning of the experiment. Then, the algae population probably increases. With higher concentration, algae may react faster to a change in lighting.

Our results also show that the algae are still active more than 8 months after their inoculation without receiving any additional nutrients, which is unusual. This long lifespan is probably due to the mixotrophic skills of this algae species (*chlorella vulgaris*): the surviving individuals extracting their nutrients from the ones that already died. Despite an evolution of the source of the nutrients during the experiments, we do not measure any change with time of the discrimination factors.

https://doi.org/10.5194/egusphere-2026-1369
Preprint. Discussion started: 8 April 2026

4.2.Comparison of our values for $^{18}\varepsilon_{dark}$ and $^{18}\varepsilon_{light}$ with previous determinations

Combining results from our new study to previous studies, we present in Table 4 a compilation of the discrimination factors obtained for aquatic species, both for respiration and photosynthesis, for different organisms and experimental conditions, ranging from laboratory conditions (in vitro or incubation experiments) to sampling in lakes or in the open ocean. Laboratory experiments measured discrimination factors between -17 and -26 ‰ including the different types of respiration, and between 0 and +6 ‰ for photosynthesis *(Guy et al., 1993; Helman et al., 2005; Eisenstadt et al., 2010).* On larger scale natural communities, discrimination factors for respiration were measured ranging from -19 to -25 ‰ with even some values below -30 ‰ *(Kroopnick and Craig, 1972; Luz et al., 2002; Hendricks et al., 2004; Luz and Barkan, 2011; Luz et al., 2014; Musan et al., 2024).*

Table 4: comparison of several studies who measured discrimination factors for respiration ($^{18}\varepsilon_{respi}$) and photosynthesis ($^{18}\varepsilon_{photo}$) in various conditions

Year	Main author(s) and year of publication	$^{18}\varepsilon$respi (‰)	$^{18}\varepsilon$photo (‰)	Temperature (°C)	species	Experiment Conditions
1993	Guy et al. (1993)		0.62 ± 0.23		diatoms	blocked photorespiration + Bubbling with Helium
1993	Quay et al. (1995)	-22				global uptake estimates in subarctic Pacific
1995	Quay et al. (1995)	-17,6			bacteria	global uptake estimates in Amazon River, O2 uptake dominated by bacteria
2002	Luz and Barkan (2002)	-21.6			plankton community dominated by phytoplankton	incubation experiments with natural plankton in Lake Kinneret
2002	Luz and Barkan (2002)	-22 to -25			plankton community dominated by phytoplankton	global uptake estimates on Lake Kinneret
2004	Hendricks 2004	-21 +/-2		0 to 10	mix	global uptake estimates on Equatorial Pacific
2004	Hendricks 2004	-22+/-1		0 to 10	mix	global uptake estimates on Southern Ocean
2005	Helman 2005	-17.1		30 or room temperature?	bacteria	bacteria from lake Kinneret blocked photorespiration with very low dissolved O2 (<3uM) +Bubbling with Helium

https://doi.org/10.5194/egusphere-2026-1369
Preprint. Discussion started: 8 April 2026

2005	Helman 2005	-19.4	+0.47	30 or room temperature?	cyanobacteria	freshwater cyanobacteria at cell level in lab blocked photorespiration with very low dissolved O2 (<3uM) +Bubbling with Helium
2007	Reuer	-25.2 +/-1.9			mix/unknown	average calculation for global ocean from numerous data points, but no measurements of fractionation
2010	Eisenstadt 2010		0.4 ± 0.03	30	cyanobacteria	blocked photorespiration with very low dissolved O2 (<3uM) +Bubbling with Helium
2010	Eisenstadt 2010		+7.04 ± 0.10	22	green algae	blocked photorespiration with very low dissolved O2 (<3uM) +Bubbling with Helium
2010	Eisenstadt 2010		+2.85 ± 0.05	18 to 20	microalgae	blocked photorespiration with very low dissolved O2 (<3uM) +Bubbling with Helium
2010	Eisenstadt 2010		+4.43 ± 0.01	18 to 20	diatoms	blocked photorespiration with very low dissolved O2 (<3uM) +Bubbling with Helium
2010	Eisenstadt 2010		+5.81 ± 0.06	18 to 20	coccolithophores	blocked photorespiration with very low dissolved O2 (<3uM) +Bubbling with Helium
2011	Luz and Barkan (2011)	-20.6 to 22.8	+0.8 to +2.6	21.6 to 25.3	mix/unknown	estimated global fractionations from in situ open water samplings in the Red Sea Near Eilat
2011	Luz and Barkan (2011)	-20.9 to 24.0	+0.7 to +3.7	19.3 to 26.5	mix/unknown	estimated global fractionations from in situ open water samplings in the North Atlantic Near Bermuda
2011	Luz and Barkan (2011)	-27.2 ± 0.8	+3.4 ± 0.2	11.2	mix/unknown	estimated global fractionations from in situ open water samplings in the Celtic Sea, Prebloom
2011	Luz and Barkan (2011)	-26.0 ± 1.4	+4.2 ± 0.4	11.5	mix/unknown	estimated global fractionations from in situ open water samplings in the Celtic Sea, bloom
2011	Luz and Barkan (2011)	-26.9 ± 0.8	+5.7 ± 0.5	3.6	mix/unknown	estimated global fractionations from in situ open water samplings in the Southern Ocean (Eisenex Experiment) Without Fe

https://doi.org/10.5194/egusphere-2026-1369
Preprint. Discussion started: 8 April 2026

2011	Luz and Barkan (2011)	-26.7 ± 0.3	+5.4 ± 0.3	3.6	mix/unknown	estimated global fractionations from in situ open water samplings in the Southern Ocean (Eisenex Experiment) With Fe
2014	Luz et al. (2014)			NA	NA	Review chapter, no measurements
2018	Stolper et al. (2018)	-13.9 to -17		15 to 37	E. Coli	lab incubation in sterile medium (salts, vitamins and trace elements)
2024	Musan et al. (2024)	-18.9 to -24.0		6	mix/unknown	in situ or lab incubations, with or without air bubbling
2024	Musan et al. (2024)	-13.9 to -23.0		around 5	mix/unknown	open water, in situ measurement of O2 and d18O, and calculation of isotopic effect (=discrimination ratio) for water column by deducing sediment oxygen uptake
	Bienville et al. (this study)	-31±5	-5	25	Chlorella vulgaris	lab incubation in aquatic microcosms and dynamic measurements of air O2 composition

As we can see from this table, the published values for the discrimination factors at respiration range from -7 to -27 ‰, hence smaller than our determination (-31±5 ‰). However, it can be noted that in their review, Luz et al. (2014) also present some values below -30 ‰ from measurements in the Southern Ocean from Reuer et al. (2007). We explore here the reasons why our determination is higher than previous studies.

A first possibility would be a problem with our system. Because our atmosphere reservoir is rather small, we are sensitive to leaks in the system. In supplementary materials, we evaluate the impact of a leak on our results and conclude that a leak would not explain an overestimation of the discrimination factor for respiration.

Another possible explanation for the observed differences lies in the experimental conditions of our experiences. Indeed, we worked at a relatively high temperature (25°C) and sometimes high CO_2 concentrations. Stolper (2018) already demonstrated a dependency between the temperature of the experimental conditions and the fractionation factors, higher temperatures being associated with stronger fractionation factors. Although their results were obtained from E. coli, the translation of this phenomenon to phytoplankton species could explain why our values are at the higher limit of previous published values. Such an hypothesis should be tested in a follow up study using a variable temperature for our experiments. Similarly, the CO_2 concentration has been shown to influence the ^{13}C discrimination between plant and atmosphere during both photosynthesis and respiration (Jacotot et al., 2021). We can wonder here if the modification of the composition of the atmosphere in our closed chamber leading to periods with high (or low) concentrations of CO_2 or O_2 can also influence our ^{18}O discrimination. Answering this question requires further experiments led under controlled CO_2 concentration.

Finally, we studied only one aquatic species in our experiments, and it was a mixotrophic species which might have more complex fractionation processes in later stages of the experiment when there were less nutrients. To address this issue, a follow up study should run experiments using autotrophic-only algae instead of mixotrophic algae.

Regarding photosynthetic discrimination, our estimate is lower than the latest estimates although being associated with a large uncertainty. The previous study of Eisenstadt (2010) measured the dissolved O_2 inside the water, whereas we measured the O_2 concentration directly in the atmosphere for more direct implication for the Dole-Morita Effect calculation. For respiration there is

https://doi.org/10.5194/egusphere-2026-1369
Preprint. Discussion started: 8 April 2026

no correction needed as we both measure the dynamics in O_2, albeit in different phases. However, photosynthesis calculations include the isotopic composition of water, so in order to compare our results we should first correct for the additional fractionation due to the transfer from dissolved O_2 to atmospheric O_2. According to the equation of Benson et al. (1984) this fractionation is of +0.7 ‰. Finally the precision of our results remains too low to provide a robust determination of the fractionation factor, or to test the existence or absence of a fractionation during photosynthesis. Future studies should hence include longer light periods with a higher number of measurement points for O_2 concentration and isotopic composition in each phase. Running longer experiments in light periods was not possible in our set-up because the CO_2 concentration was too low at the end of the light periods. A next version of our set-up should probably include a system for some CO_2 regulation.

5.Conclusion

In this study, we built a simplified set-up to study the fluxes of O_2 and CO_2 during respiration and photosynthesis for the aquatic biosphere. This closed biological chamber equipped with numerous sensors and a system for regular air sampling is validated through experiments performed with *chlorella vulgaris,* a freshwater phytoplankton species. These first experiments allowed us to measure significant changes of concentration and isotopic composition of O_2 later used for the determination of biological fractionation factors.

We obtained a fractionation discrimination of 31±5 ‰ for respiration, which is at the highest limit of previous estimates using different experimental set-ups. These high values may be explained by the relatively high temperature (23-25°C) during our experiments or by the particular behaviour of the mixotrophic algae chosen here after a few weeks of incubation.

The photosynthetic fractionation discrimination values obtained here show a large scattering and a slightly negative mean value which does not agree with the most recent determination. We suggest further experiments with longer light periods which will only be possible if we modify our set-up to be able to add CO_2 in the system during the course of the experiment.

As a perspective, several improvements and extensions to this experimental setup would strengthen its relevance and applicability. In particular, implementing active CO_2 control would enable more stable atmospheric concentrations in order to better simulate more realistic conditions, while also offering the flexibility to study the whole biological set-up and fractionation factors at different CO_2 levels, useful for simulating past atmosphere composition. We also plan to expand our investigation to include other phytoplankton species, particularly diatoms, which would provide a more comprehensive picture of global O_2 production dynamics, as these organisms collectively dominate marine primary productivity. Finally, systematically examining the temperature dependence of the observed processes would be crucial, given the sensitivity of both photosynthetic rates and gas exchange kinetics to thermal conditions—insights that are particularly relevant in the context of ongoing climate change.

Code and data availability

The data used in this study are included in the paper either with figures or tables, or in the Supplement. The python code used for the controlling the experiments is available at https://gitlab.in2p3.fr/olivier.jossoud/aquaoxy/-/tree/paper_2025.

Author contributions

AL, CP and SF designed the project and acquired the funding. FP, AD, NG, BL, SF, SC, JC and NB all contributed to design and build the system presented, and all authors provided resources in the process. OJ created the computer program running the

https://doi.org/10.5194/egusphere-2026-1369
Preprint. Discussion started: 8 April 2026

experiment. NB performed the experiments, collected and cured the data, and did the data visualization. NB and AL wrote the manuscript, with contributions from SF, JS, SA and CP.

Competing interests

The authors declare that they have no conflict of interest.

Acknowledgements

The research leading to these results has received funding from the European Research Council under the European Union H2020 Programme (H2020/20192024)/ERC grant agreement no. 817493 (ERC ICORDA), from ANR HUMI17, from the PhD grant 80PRIME from CNRS and from the AQUAOXY project.

This study also benefited from the CNRS resources allocated to the French ECOTRONS Research Infrastructure, and FEDER investments as well as from the state allocation "Investissement d'Avenir" AnaEE-France ANR-11-INBS-0001. The authors also acknowledge the scientific and technical support of PANOPLY (Plateforme ANalytique géOsciences Paris-sacLaY), Paris-Saclay University, France and CEREEP écotronIDF.

Finally, we would also like to thank for their help Francis Dohou, Didier Jehanno and Emilie Cantin from CEREEP Ecotron-IDF, and Laurence Vialettes Bruno Bombled and Elodie Brugere from Laboratoire des Sciences du Climat et de l'Environnement.

References

Angert, A., Yakir, D., Rodeghiero, M., Preisler, Y., Davidson, E. A., and Weiner, T.: Using O_2 to study the relationships between soil CO_2 efflux and soil respiration, Biogeosciences, 12, 2089–2099, https://doi.org/10.5194/bg-12-2089-2015, 2015.

Barkan, E. and Luz, B.: High precision measurements of^{17} O/^{16} O and^{18} O/^{16} O ratios in H_2 O, Rapid Comm Mass Spectrometry, 19, 3737–3742, https://doi.org/10.1002/rcm.2250, 2005.

Bender, M., Grande, K., Johnson, K., Marra, J., Williams, P. J. LeB., Sieburth, J., Pilson, M., Langdon, C., Hitchcock, G., Orchardo, J., Hunt, C., Donaghay, P., and Heinemann, K.: A comparison of four methods for determining planktonic community production1, Limnology & Oceanography, 32, 1085–1098, https://doi.org/10.4319/lo.1987.32.5.1085, 1987.

Bender, M., Sowers, T., and Labeyrie, L.: The Dole Effect and its variations during the last 130,000 years as measured in the Vostok Ice Core, Global Biogeochemical Cycles, 8, 363–376, https://doi.org/10.1029/94GB00724, 1994.

Benson, B. B. and Krause, D.: The concentration and isotopic fractionation of oxygen dissolved in freshwater and seawater in equilibrium with the atmosphere', 620–632, 1984.

Bereiter, B., Eggleston, S., Schmitt, J., Nehrbass-Ahles, C., Stocker, T. F., Fischer, H., Kipfstuhl, S., and Chappellaz, J.: Revision of the EPICA Dome C CO_2 record from 800 to 600 kyr before present, Geophysical Research Letters, 42, 542–549, https://doi.org/10.1002/2014GL061957, 2015.

Dole, M.: THE RELATIVE ATOMIC WEIGHT OF OXYGEN IN WATER AND IN AIR, J. Am. Chem. Soc., 57, 2731–2731, https://doi.org/10.1021/ja01315a511, 1935.

Eisenstadt, D., Barkan, E., Luz, B., and Kaplan, A.: Enrichment of oxygen heavy isotopes during photosynthesis in phytoplankton, Photosynth Res, 103, 97–103, https://doi.org/10.1007/s11120-009-9518-z, 2010.

Guy, R. D.: Photosynthetic Fractionation of the Stable lsotopes of Oxygen and Carbon', 101, 1993.

Harris Stuart, R., Landais, A., Arnaud, L., Buizert, C., Capron, E., Dumont, M., Libois, Q., Mulvaney, R., Orsi, A., Picard, G., Prié, F., Severinghaus, J., Stenni, B., and Martinerie, P.: On the relationship between δ O_2 /N_2 variability and ice sheet surface conditions in Antarctica, The Cryosphere, 18, 3741–3763, https://doi.org/10.5194/tc-18-3741-2024, 2024.

Hayes, J. M.: Practice and Principles of Isotopic Measurements in Organic Geochemistry, 2002.

https://doi.org/10.5194/egusphere-2026-1369
Preprint. Discussion started: 8 April 2026

Helman, Y., Barkan, E., Eisenstadt, D., Luz, B., and Kaplan, A.: Fractionation of the Three Stable Oxygen Isotopes by Oxygen-Producing and Oxygen-Consuming Reactions in Photosynthetic Organisms, Plant Physiology, 138, 2292–2298, https://doi.org/10.1104/pp.105.063768, 2005.

Hendricks, M. B., Bender, M. L., and Barnett, B. A.: Net and gross O2 production in the southern ocean from measurements of biological O2 saturation and its triple isotope composition, Deep Sea Research Part I: Oceanographic Research Papers, 51, 1541–1561, https://doi.org/10.1016/j.dsr.2004.06.006, 2004.

Hillaire-Marcel, C., Kim, S.-T., Landais, A., Ghosh, P., Assonov, S., Lécuyer, C., Blanchard, M., Meijer, H. A. J., and Steen-Larsen, H. C.: A stable isotope toolbox for water and inorganic carbon cycle studies, Nat Rev Earth Environ, 2, 699–719, https://doi.org/10.1038/s43017-021-00209-0, 2021.

Intergovernmental Panel On Climate Change (Ipcc): Climate Change 2021 – The Physical Science Basis: Working Group I Contribution to the Sixth Assessment Report of the Intergovernmental Panel on Climate Change, 1st ed., Cambridge University Press, https://doi.org/10.1017/9781009157896, 2023.

Ishidoya, S., Sugawara, S., and Okazaki, A.: Diurnal, seasonal, and interannual variations in δ (^{18} O) of atmospheric O_2 and its application to evaluate natural and anthropogenic changes in oxygen, carbon, and water cycles, Atmos. Chem. Phys., 25, 1965–1987, https://doi.org/10.5194/acp-25-1965-2025, 2025.

Jacotot, A., Marchand, C., Gayral, I., and Allenbach, M.: Effects of Elevated CO2 Concentrations on 13C Fractionation during Photosynthesis, Post-Photosynthesis and Night Respiration in Mangrove Saplings Avicennia marina and Rhizophora stylosa, Wetlands, 41, 62, https://doi.org/10.1007/s13157-021-01461-2, 2021.

Keeling, R. F. and Manning, A. C.: Studies of Recent Changes in Atmospheric O2 Content, in: Treatise on Geochemistry, Elsevier, 385–404, https://doi.org/10.1016/B978-0-08-095975-7.00420-4, 2014.

Kiddon, J., Bender, M. L., Orchardo, J., Caron, D. A., Goldman, J. C., and Dennett, M.: Isotopic fractionation of oxygen by respiring marine organisms, Global Biogeochemical Cycles, 7, 679–694, https://doi.org/10.1029/93GB01444, 1993.

Kilham, S. S., Kreeger, D. A., Lynn, S. G., Goulden, C. E., and Herrera, L.: COMBO: a defined freshwater culture medium for algae and zooplankton, 1998.

Kroopnick, P. and Craig, H.: Atmospheric Oxygen: Isotopic Composition and Solubility Fractionation, Science, 175, 54–55, https://doi.org/10.1126/science.175.4017.54, 1972.

Landais, A., Dreyfus, G., Capron, E., Masson-Delmotte, V., Sanchez-Goñi, M. F., Desprat, S., Hoffmann, G., Jouzel, J., Leuenberger, M., and Johnsen, S.: What drives the millennial and orbital variations of δ18Oatm?, Quaternary Science Reviews, 29, 235–246, https://doi.org/10.1016/j.quascirev.2009.07.005, 2010.

Lane, G. A. and Dole, M.: Fractionation of Oxygen Isotopes during Respiration, Science, 123, 574–576, https://doi.org/10.1126/science.123.3197.574, 1956.

Luz, B. and Barkan, E.: Assessment of Oceanic Productivity with the Triple-Isotope Composition of Dissolved Oxygen, Science, 288, 2028–2031, https://doi.org/10.1126/science.288.5473.2028, 2000.

Luz, B. and Barkan, E.: The isotopic composition of atmospheric oxygen: ISOTOPIC COMPOSITION OF AIR OXYGEN, Global Biogeochem. Cycles, 25, n/a-n/a, https://doi.org/10.1029/2010GB003883, 2011.

Luz, B., Barkan, E., Sagi, Y., and Yacobi, Y. Z.: Evaluation of community respiratory mechanisms with oxygen isotopes: A case study in Lake Kinneret, Limnology & Oceanography, 47, 33–42, https://doi.org/10.4319/lo.2002.47.1.0033, 2002.

Luz, B., Barkan, E., and Severinghaus, J. P.: The Stable Isotopic Composition of Atmospheric O2, in: Treatise on Geochemistry, Elsevier, 363–383, https://doi.org/10.1016/B978-0-08-095975-7.00419-8, 2014.

Morita, V. N. and Titani, T.: UBER DEN UNTERSCHIED DER ISOTOPENZUSAMMEN- SETZUNG VON LUFT- UND, 1935.

https://doi.org/10.5194/egusphere-2026-1369
Preprint. Discussion started: 8 April 2026

Musan, I., Gildor, H., Gonsiorczyk, T., Grossart, H., and Luz, B.: Isotope effects of O_2 consumption in a deep lake as means for understanding partitioning of O_2 demand among microorganisms, particles, and sediment, Limnology & Oceanography, 69, 992–1004, https://doi.org/10.1002/lno.12543, 2024.

Paul, C., Piel, C., Sauze, J., Pasquier, N., Prié, F., Devidal, S., Jacob, R., Dapoigny, A., Jossoud, O., Milcu, A., and Landais, A.: Determination of respiration and photosynthesis fractionation factors for atmospheric dioxygen inferred from a vegetation–soil–atmosphere analogue of the terrestrial biosphere in closed chambers, Biogeosciences, 20, 1047–1062, https://doi.org/10.5194/bg-20-1047-2023, 2023.

Paul, C., Piel, C., Sauze, J., Jossoud, O., Dapoigny, A., Romanini, D., Prié, F., Devidal, S., Jacob, R., Milcu, A., and Landais, A.: A multiplexing system for quantifying oxygen fractionation factors in closed chambers, Geosci. Instrum. Method. Data Syst., 14, 91–101, https://doi.org/10.5194/gi-14-91-2025, 2025a.

Paul, C., Piel, C., Sauze, J., Yang, J.-W., Bouchet, M., Jossoud, O., Dapoigny, A., Romanini, D., Prié, F., Devidal, S., Jacob, R., Milcu, A., and Landais, A.: Air oxygen fractionation associated with respiration and photosynthesis processes in plants: impact on the study of the global Dole effect, Quaternary Science Reviews, 370, 109663, https://doi.org/10.1016/j.quascirev.2025.109663, 2025b.

Piel, C., Romanini, D., Farradèche, M., Chaillot, J., Paul, C., Bienville, N., Lauwers, T., Sauze, J., Jaulin, K., Prié, F., and Landais, A.: High-precision oxygen isotope (δ^{18} O) measurements of atmospheric dioxygen using optical-feedback cavity-enhanced absorption spectroscopy (OF-CEAS), Atmos. Meas. Tech., 17, 6647–6658, https://doi.org/10.5194/amt-17-6647-2024, 2024.

Quay, P. D., Wilbur, D. ., Richey, J. E., Devol, A. H., Benner, R., and Forsberg, B. R.: The 18O:16O of dissolved oxygen in rivers and lakes in the Amazon Basin: Determining the ratio of respiration to photosynthesis rates in freshwaters, Limnol. Oceanogr., 40, 718–729, https://doi.org/10.4319/lo.1995.40.4.0718, 1995.

Reuer, M. K., Barnett, B. A., Bender, M. L., Falkowski, P. G., and Hendricks, M. B.: New estimates of Southern Ocean biological production rates from O2/Ar ratios and the triple isotope composition of O2, Deep Sea Research Part I: Oceanographic Research Papers, 54, 951–974, https://doi.org/10.1016/j.dsr.2007.02.007, 2007.

Severinghaus, J. and Battle, M.: Fractionation of gases in polar ice during bubble close-off: New constraints from firn air Ne, Kr and Xe observations, Earth and Planetary Science Letters, 244, 474–500, https://doi.org/10.1016/j.epsl.2006.01.032, 2006.

Stolper, D. A., Fischer, W. W., and Bender, M. L.: Effects of temperature and carbon source on the isotopic fractionations associated with O2 respiration for 17O/16O and 18O/16O ratios in E. coli, Geochimica et Cosmochimica Acta, 240, 152–172, https://doi.org/10.1016/j.gca.2018.07.039, 2018.

Tcherkez, G., Gauthier, P., Buckley, T. N., Busch, F. A., Barbour, M. M., Bruhn, D., Heskel, M. A., Gong, X. Y., Crous, K. Y., Griffin, K., Way, D., Turnbull, M., Adams, M. A., Atkin, O. K., Farquhar, G. D., and Cornic, G.: Leaf day respiration: low CO_2 flux but high significance for metabolism and carbon balance, New Phytologist, 216, 986–1001, https://doi.org/10.1111/nph.14816, 2017.

Wostbrock, J. A. G., Cano, E. J., and Sharp, Z. D.: An internally consistent triple oxygen isotope calibration of standards for silicates, carbonates and air relative to VSMOW2 and SLAP2, Chemical Geology, 533, 119432, https://doi.org/10.1016/j.chemgeo.2019.119432, 2020.